Journal of Solid State Chemistry **150,** 347–355 (2000)
doi:10.1006/jssc.1999.8601, available online at http://www.idealibrary.com on IDEAL®

Structure–Composition Relations and Fractional Site Occupancy of New M_5Ge_4 Compounds in the System Ge–Ta–Zr

Klaus W. Richter*,[1] and H. Fritz Franzen†

*Institut fur anorganische Chemie, Universität Wien, Währingerstrasse 42, A-1090 Wien, Austria; and †Ames Laboratory and Department of Chemistry, Iowa State University, Ames, Iowa 50011

Received October 5, 1999; in revised form November 29, 1999; accepted December 4, 1999

The new ternary phases $Zr_{4-x}Ta_{1+x}Ge_4$ ($0.1 < x < 0.4$) and $Zr_{2+x}Ta_{3-x}Ge_4$ ($0.1 < x < 1.1$) were prepared from the elements by arc melting and subsequent induction heating at 1400–1450°C. Single-crystal X-ray diffraction was used to determine their structures and to refine mixed site occupancies. $Zr_{4-x}Ta_{1+x}Ge_4$ was found to crystallize in the monoclinic space group $P2_1/c$ (structure type: $U_2Mo_3Si_4$) and the compound $Zr_{2-x}Ta_{3-x}Ge_4$ shows orthorhombic symmetry (space group *Pnma*, structure type: Sm_5Ge_4). The close structural relationship between the two structures is discussed. Both phases exhibit pronounced differential fractional site occupancy of Ta and Zr on the metal sites and considerable composition ranges. Extended Hückel calculations were performed for various site occupancy models and Mulliken overlap populations for the different lattice sites of each structure were calculated for these models. The correlation of the cumulated Mulliken overlap populations and the atomic orbital populations with the actual site occupancies is discussed. © 2000 Academic Press

Key Words: **tantalum zirconium germanides; crystal structure; bonding; disorder; differential fractional site occupancy.**

INTRODUCTION

Ternary compounds of the type $M_xM'_yX$, where M and M' are two early transition metals of group 4 or 5 of the periodic system and X is S or P, were reported to exhibit special structural features closely related to the similarity of the two metal atoms. In the ternary Nb–Ta–S system, for instance, four metal-rich ternary compounds have been reported: $(Nb_{0.45}Ta_{0.55})_{11}S_4$ (1), $(Nb_{0.56}Ta_{0.44})_{12}S_4$ (2), $(Nb_{0.34}Ta_{0.66})_5S_2$ (3), and $Nb_{0.95}Ta_{1.05}S$ (4). In spite of the close similarity of Nb and Ta, all of these compounds, except $Nb_{0.95}Ta_{1.05}S$, show structures that are unique for these special combinations of elements and are unknown in the limiting binary systems. The special features observed in these compounds led to a new chemical concept of the stabilization of partially ordered solid solution phases by differential fractional site occupation (5). Defining characteristics for compounds stabilized by differential fractional site occupancy (DFSO) given by Franzen and Köckerling (6) include mixed site occupancies on the metal sites combined with pronounced site preferences of the metals on different sites (i.e., a variation of the observed metal ratio from site to site). The phases are thus influenced by the competing factors of entropic stabilization due to the mixed site occupation and differences in the bonding capability between the different metals yielding different metal ratios for different sites. Some new mixed transition metal compounds have been prepared in ternary systems of the early transition metals with elements of groups 15 and 16 through the application of the differential fractional site occupation concept, including, e.g., $Hf_{10}Ta_3S_3$ (7) and $Hf_{5.08}Mo_{0.92}P_3$ (8).

The work presented here is part of a current research project with the aim to prepare and structurally characterize possible new compounds in mixed early transition metal–germanium systems and to discuss their fractional site occupancies in the context of the DFSO-concept. Some isothermal sections in mixed transition metal–germanium systems like Ge–Hf–Nb (9) or Ge–V–Zr (10) have been studied by Seropegin and co-workers showing the existence of ternary phases in these systems without giving detailed structural information. These studies, however, were carried out at 800 and 900°C, which is a rather low temperature for entropy stabilized DFSO-materials and are thus of limited value for the current study. No information about phase diagrams or ternary compounds could be found for the system Ge–Ta–Zr, which was selected for a detailed survey in the current study.

EXPERIMENTAL

Sample Preparation

The samples were prepared from Ge powder (99.999%, Alfa AESAR), Ta powder (99.98%, Alfa AESAR), and Zr

[1]To whom correspondence should be addressed. E-mail: richter@ap.univie.ac.at.

0022-4596/00 $35.00

powder (99.7% Alfa AESAR). Samples for single-crystal investigations were prepared using high-purity Zr rod (99.99%, Ames Lab, IA). The metal powders were handled in an Ar-filled dry box. Calculated amounts of the element powders were weighed to an accuracy of approximately 0.5 mg, mixed carefully, pressed into 8-mm pellets under a load of 4 metric tons and then arc-melted on a water-cooled copper hearth in an argon atmosphere. The obtained reguli with a total mass of about 1000 mg were remelted two times for homogenization and then weighed back in order to check for possible mass losses. Weight losses of 1–2.5% during the arc-melting process were attributed to the evaporation of germanium and were compensated by the addition of extra germanium powder to the initial sample mixtures. For equilibration and crystal growth the reguli were subsequently annealed for 40 h by induction heating in a tungsten crucible at 1400–1450°C in a dynamic vacuum of $p < 2 \times 10^{-6}$ Torr.

Powder Diffraction

Powder patterns were obtained with an Enraf–Nonius Guinier chamber using monochromated Cu$K\alpha$ radiation and employing an internal standard of high purity Si. The patterns of the new ternary phases were initially observed in samples with the nominal compositions $Zr_{35}Ta_{15}Ge_{50}$ and $Zr_{25}Ta_{25}Ge_{50}$. Subsequently, a systematic study of the powder patterns in two sample series at 50 and 45 at% Ge, respectively, was carried out in order to determine the composition range of the ternary phases. In agreement with the M_5Ge_4 stoichiometry of the ternary phases, almost pure powder patterns of $Zr_{4-x}Ta_{1+x}Ge_4$ and $Zr_{2+x}Ta_{3-x}Ge_4$ could be observed in the sample series at 45 at% Ge. Weak additional lines, mainly of W_5Si_3- and Mn_5Si_3-type $(Zr,Ta)_5Ge_3$ phases were apparently due to inhomogeneities in the samples and Ge-losses during the annealing procedure. Variation of the germanium to metal ratio finally yielded in the preparation of pure orthorhombic $Zr_{2+x}Ta_{3-x}Ge_4$. The monoclinic phase $Zr_{4-x}Ta_{1+x}Ge_4$ could be prepared with a yield of more than 90%, but not entirely pure, which is probably due to an incongruent melting behavior of the phase yielding inhomogeneities within the sample that could not be overcome completely during the annealing procedure.

Microprobe Analysis

In order to determine accurate phase compositions, possible inhomogeneities, and additional impurity phases, four of the samples were investigated with an electron microprobe (ARL SEMQ) equipped with three scanning spectrometers. Measurements were performed at 20-kV acceleration voltage and 5-nA electron beam current using the characteristic Lα radiation of Ge, Zr, and Ta for analysis. The results of these measurements were in excellent agreement with the phase compositions observed by powder diffraction and the empirical formula found by single-crystal data refinement.

Single-Crystal X-Ray Diffraction

Single-crystal data were collected with a Bruker-AXS CCD-1000 diffractometer using Mo$K\alpha$ radiation and a diffractometer to crystal distance of 5.08 cm. Initial cell constants were obtained from 60 frames in three series of ω-scans at different starting angles. The reflections were indexed by an automatic index routine. Data collection included three sets of frames with 0.3° scans in ω with an exposure time of 30 s per frame. The total number of frames collected was 1271. Peak integration was performed using the SAINT program, and final lattice constants were obtained by least-squares fits of the entire data set. The absorption correction was based on a ψ-scan routine of the program XPREP using all data with $I > 20\sigma$. All software used for data processing and structure refinement is contained in the SMART/SAINT/SHELXTL (5.1) program library (11). Crystal structure and refinement data as well as final atomic parameters for all three compounds listed below are given in Tables 1 and 2, respectively. A brief summary of unique aspects of the crystallography for the different compounds follows.

$Zr_{3.90}Ta_{1.10}Ge_4$

Single crystals were picked from a crushed sample of the nominal composition $Zr_{35}Ta_{15}Ge_{50}$ with a powder pattern showing small amounts of additional phases. The crystals were mounted in thin-wall glass capillaries and sealed in air. The crystal quality was checked with Laue photographs and a crystal of approximate dimensions $0.1 \times 0.07 \times 0.05$ mm (no clear morphology) was chosen for data collection. The observed reflections could be indexed with a monoclinic cell of dimensions $a = 7.126$, $b = 7.116$, $c = 6.919$ Å, and $\beta = 109.35°$. Systematic absences of the reflections $h0l$ ($l \neq 2n$), $0k0$ ($k \neq 2n$), and $00l$ ($l \neq 2n$) (1 very weak exception) left $P2_1/c$ as the only possible choice for the space group. The application of direct methods gave all five independent atom positions. Subsequent refinement cycles with isotropic thermal parameters proceeded smoothly, but unreasonable thermal parameters for $M1$ and $M2$ revealed possible fractional site occupancies. Mixed Ta/Zr positions were thus allowed first for position $M1$ and in a second step on position $M2$ with the condition that the sum of Ta and Zr occupancies equals one. This procedure yielded reasonable isotropic thermal parameters for $M1$ and $M2$. The possibility of fractional occupancies was also tested for $M3$ but the deviation of the site occupation from unity was insignificant and the site occupancy of $M3$ was therefore

TABLE 1
Selected Data Collection and Refinement Parameters

	$Zr_{3.90}Ta_{1.10}Ge_4$	$Zr_{3.13}Ta_{1.87}Ge_4$	$Zr_{3.98}Ta_{1.02}Ge_4$
Crystal system, space group	monoclinic, $P2_1/c$	orthorhombic, *Pnma*	tetragonal, $P4_12_12$
Cell dimensions, a/Å	7.126(1)	6.880(2)	7.1416(8)
b/Å	7.116(1)	13.389(4)	7.1416(8)
c/Å	6.919(1)	7.003(2)	13.067(2)
β/°	109.350(3)	90.0	90.0
V/Å^3	331.0(1)	645.1(3)	666.4(2)
Formula units Z	2	4	4
Reflections collected, unique	1994, 767	3825, 806	4397, 833
Parameters refined	46	48	44
Extinction coefficient	0.0074	—	—
R, R_w for $I > 2\sigma(I)$	0.0289, 0.0596	0.0312, 0.0706	0.0278, 0.0571
R, R_w for all data	0.0373, 0.0615	0.0425, 0.0750	0.0363, 0.0592

Note. $R = \sum \| F_o| - |F_c\| / \sum |F_o|$, $R_w = [\sum w(|F_o| - |F_c|)^2 / \sum w(F_o)^2]^{1/2}$, $w = 1/(\sigma^2 F_o^2 + (\text{axP})^2 + (\text{bxP}))$.

assigned as pure Zr in the final refinement. The Fourier difference map after final anisotropic refinement showed no residual peaks larger than 1.8 and -1.9 e/Å^3. The structure was recognized as a partially disordered form of the $U_2Mo_3Si_4$ structure type.

$Zr_{3.13}Ta_{1.87}Ge_4$

A single crystal with no clear morphology and approximate dimensions $0.13 \times 0.08 \times 0.05$ mm was picked from a crushed sample of the nominal composition $Zr_{35}Ta_{20}Ge_{45}$. The powder pattern of this sample showed essentially pure $Zr_{3.13}Ta_{1.87}Ge_4$ with few very weak additional lines of the monoclinic phase $Zr_{4-x}Ta_{1+x}Ge_4$. After checking the crystal quality using the Laue technique, single data were collected on the CCD diffractometer. The observed reflections could be indexed assuming an orthorhombic cell of dimensions $a = 6.880$, $b = 13.389$, and $c = 7.003$ Å.

Systematic absences of reflections with $0kl$ ($k + l \neq 2n$), $hk0$ ($h \neq 2n$), $h00$ ($h \neq 2n$), $0k0$ ($k \neq 2n$), and $00l$ ($l \neq 2n$) were consistent with space groups *Pnma* and $Pna2_1$. Refinement in the centrosymmetric space group *Pnma* was successful. The application of direct methods revealed six atom

TABLE 2
Positional Parameters and Site Occupancies

Atom	Occupation	Symmetry	x	y	z	U_{eq}/Å^2
$Zr_{3.90}Ta_{1.10}Ge_4$, $P2_1/c$						
*M*1	0.64 Ta + 0.36 Zr	2*a*:$\bar{1}$	0	0	0	0.013(1)
*M*2	0.23 Ta + 0.77 Zr	4*e*:1	0.2497(1)	0.3234(1)	0.2556(1)	0.013(1)
*M*3	1.00 Zr	4*e*:1	0.6886(1)	0.3277(1)	0.0584(1)	0.014(1)
Ge1		4*e*:1	0.0162(2)	0.6317(1)	0.1355(1)	0.014(1)
Ge2		4*e*:1	0.4190(2)	0.0294(1)	0.1516(1)	0.015(1)
$Zr_{3.13}Ta_{1.87}Ge_4$, *Pnma*						
*M*1	0.90 Ta + 0.10 Zr	4*c*:.*m*.	0.1679(1)	$\frac{1}{4}$	0.0062(1)	0.022(1)
*M*2	0.50 Ta + 0.50 Zr	8*d*:1	0.3420(1)	0.1250(1)	0.3309(1)	0.022(1)
*M*3	1.00 Zr	8*d*:1	0.0099(1)	0.0939(1)	0.6757(1)	0.022(1)
Ge1		4*c*:.*m*.	0.3077(2)	$\frac{1}{4}$	0.6476(2)	0.021(1)
Ge2		4*c*:.*m*.	0.0410(2)	$\frac{1}{4}$	0.3886(2)	0.022(1)
Ge3		8*d*:1	0.1836(2)	0.0396(1)	0.0353(2)	0.023(1)
$Zr_{3.98}Ta_{1.02}Ge_4$, $P4_12_12$						
*M*1	0.59 Ta + 0.41 Zr	4*a*:..2	0.3288(1)	0.3288(1)	0	0.018(1)
*M*2	0.21 Ta + 0.79 Zr	8*b*:1	0.0034(1)	0.1537(1)	0.1272(1)	0.019(1)
*M*3	1.00 Zr	8*b*:1	0.4986(1)	0.1580(1)	0.2208(1)	0.018(1)
Ge1		8*b*:1	0.1408(2)	0.2008(2)	0.3269(1)	0.019(1)
Ge2		8*b*:1	0.1982(2)	0.4615(2)	0.1834(1)	0.018(1)

sites, which were subsequently refined with isotropic thermal parameters. Due to an unreasonable small thermal parameter for Zr on the position $M2$, mixed Ta/Zr occupancy was allowed on this position. In a second step, mixed occupancies were also refined on position $M1$ yielding reasonable isotropic thermal parameters for $M1$ and $M2$ as well as excellent agreement of the refined empirical formula with the nominal overall composition of the sample. $M3$ was found to be pure Zr. After final anisotropic refinement the largest residual peaks in the Fourier difference map were 2.5 and -1.4 e/Å^3 at 0.86 Å from position $M1$. The structure was recognized as a partially ordered ternary variant of the Sm_5Ge_4 structure type.

$Zr_{3.98}Ta_{1.02}Ge_4$

An additional single-crystal data set was collected in order to gather information about the fractional site occupancies in the adjacent phase $Zr_{5-x}Ta_xGe_4$ (compare later sections). The crystal with the refined composition $Zr_{3.98}Ta_{1.02}Ge_4$ belongs to the ternary solid solution of Ta in binary Zr_5Ge_4 (tetragonal, $P4_12_12$, structure type: Zr_5Si_4) and marks the solubility limit of tantalum in the binary phase. The atomic positions and site occupancies were refined by a method similar to the procedure described above.

RESULTS AND DISCUSSION

The monoclinic structure type $U_2Mo_3Si_4$ has been reported in compounds of the lanthanide and actinide series, e.g., in $Ln_2Mo_3Si_4$ with Ln = Dy, Er, Ho, Tb, Tm, Y (12) and in $U_2M_3X_4$ with M = V, Mo, W and X = Si, Ge (13). According to these studies, the ternary compounds exhibit no mixed site occupancies on the metal sites and the lanthanide or actinide metal occupies only the position assigned as $M3$ in Table 2. In contrast, $Zr_{4-x}Ta_{1+x}Ge_4$ shows pronounced differential fractional site occupancies of Ta and Zr on the positions $M1$ and $M2$ yielding an overall composition that differs significantly from the ideal formula $Zr_2Ta_3Ge_4$. $Zr_{4-x}Ta_{1+x}Ge_4$ can thus be regarded as a disordered variant of the $U_2Mo_3Si_4$ structure type.

The orthorhombic structure type Sm_5Ge_4 is common in binary germanium–lanthanide systems (14) and was also found to occur in several ternary germanium systems. Most of these ternary compounds, including the series $Ln_2Nb_3Ge_4$ with Ln = Y, Gd, Tb, Dy, Ho, Er, Tm, Yb, Lu (15) and $U_2(Nb/Ta)_3Ge_4$ (16) were reported to crystallize in a totally ordered ternary variant of the Sm_5Ge_4 structure type (sometimes assigned as $Ce_2Sc_3Si_4$ type) with the lanthanide or actinide again occupying the position assigned as $M3$ in Table 2. However, a considerable homogeneity range was reported in ternary $Zr_2Nb_3Ge_4$ (17), which is obviously due to some kind of disorder on the metal positions although the totally ordered structure was found in the single-crystal refinement (18). In the present study, $Zr_{2+x}Ta_{3-x}Ge_4$ was found to exhibit mixed Ta and Zr site occupancy on the positions $M1$ and $M2$ in Table 2, yielding a shift to the Zr-rich side of the ideal ordered composition $Zr_2Ta_3Ge_4$ which could actually not be realized in the current study. $Zr_{2+x}Ta_{3-x}Ge_4$ is therefore best described as a partially ordered ternary Sm_5Ge_4 type.

The two new compounds $Zr_{4-x}Ta_{1+x}Ge_4$ and $Zr_{2+x}Ta_{3-x}Ge_4$ exhibit exact M_5Ge_4 stoichiometry with variable Ta/Zr ratios and should therefore be discussed in context with the terminating binary compound Zr_5Ge_4 (tetragonal, $P4_12_12$, structure type: Zr_5Si_4), which actually also shows limited solid solubility for Ta. It should be mentioned, that the Zr_5Si_4-structure type also occurs in an ordered ternary variant known as the $Sc_2Re_3Si_4$ type (15). The close relationship between the Zr_5Si_4 and Sm_5Ge_4 structure types has been discussed earlier (19). The structures can be described by a combination of two principal building blocks: trigonal prisms of metal atoms centered by the main group element and bcc-type fragments of metal atoms. The structures can be regarded as combinations of U_3Si_2- and FeB-like slabs. In the case of the Sm_5Ge_4 structure type there are infinite slabs stacked alternately while in Zr_5Ge_4 fragments of these slabs are arranged in a herring-bone fashion (20). The monoclinic compound $Zr_{4-x}Ta_{1+x}Ge_4$ ($U_2Mo_3Si_4$-type structure), which can also be described by a combination of trigonal prisms and bcc-type fragments, shows a remarkable similarity to the Sm_5Ge_4-type structure. For a better visualization of this similarity, the two structures are here described based upon the coordination polyhedron of the metal atom $M1$, which is situated in the center of a germanium octahedron.

Both structures can be described by layers of corner-sharing Ge octahedra, which are centered by metal atoms $M1$ and face-capped by metal atoms $M2$ and $M3$. In the case of the monoclinic compound $Zr_{4-x}Ta_{1+x}Ge_4$ (Fig. 1a) these layers are stacked regularly along the [100] direction (translational symmetry). Figure 1b shows the orthorhombic compound $Zr_{2+x}Ta_{3-x}Ge_4$ in a view 20° off [010] to give a comparable perspective. The first and second layers of octahedra are in this case, due to a doubling in the cell size, not connected by translational symmetry and are therefore slightly shifted against each other. Figure 2 shows the octahedra layers from a side view. In the case of the orthorhombic compound (Fig. 2b) the layers are perfectly flat in the xz plane according to the mirror planes situated at $y = 1/4$ and 3/4. In contrast, the layers are slightly twisted in monoclinic compound (Fig. 2a) reflecting the lack of symmetry restrictions in this case.

In summary, the two ternary phases $Zr_{4-x}Ta_{1+x}Ge_4$ and $Zr_{2+x}Ta_{3-x}Ge_4$ crystallize in two symmetrically different variants of what appears to be essentially the same structural theme. Nevertheless, the two structures are not con-

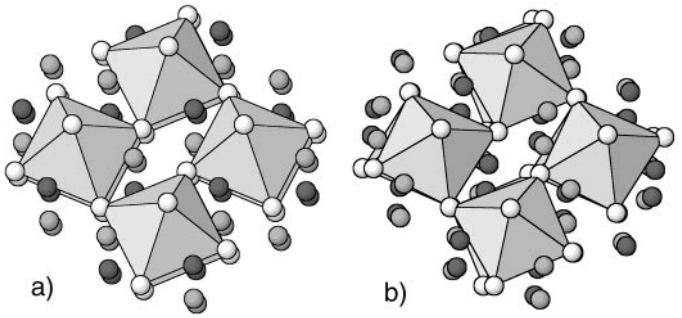

FIG. 1. (a) $Zr_{3.90}Ta_{1.10}Ge_4$, $P2_1/c$, view along [100] and (b) $Zr_{3.13}Ta_{1.87}Ge_4$, *Pnma*, view 20° off [010]. White circles, Ge; light gray, *M*2 (Ta + Zr); dark gray, *M*3 (Zr). Infinite layers of corner-sharing Ge octahedra centered by *M*1 (Ta + Zr) and face capped by *M*2 (Ta + Zr) and *M*3 (Zr). The layers are perfectly stacked in the monoclinic structure and slightly twisted in the orthorhombic case.

nected by any group–subgroup relationship, which can be seen by the fact that the orthorhombic phase exhibits higher rotational symmetry with respect to the monoclinic phase but at the same time shows lower translational symmetry due to a doubling in the cell size. Furthermore the two structures show differences in the "coloring": in the case of the monoclinic phase (Fig. 2a), the metal positions *M*2 and *M*3 (shown in light gray and dark gray in Figs. 1 and 2) are connected by the inversion center at *M*1 and therefore are situated at opposite sides of the Ge octahedra, while the two metal positions in the orthorhombic phase (Fig. 2b) are connected by mirror symmetry, and therefore they are situated at the same sides of the Ge octahedra. This fact is especially important as the two metal positions are chemically not equivalent; i.e., *M*2 is fractionally occupied by Ta and Zr while *M*3 is a pure Zr position.

The composition ranges of the two ternary phases $Zr_{4-x}Ta_{1+x}Ge_4$ and $Zr_{2+x}Ta_{3-x}Ge_4$ as well as the solid solubility of Ta in binary Zr_5Ge_4 ($Zr_{5-x}Ta_xGe_4$) were investigated by means of X-ray powder diffraction and microprobe studies using samples annealed at 1450°C. The tetragonal phase $Zr_{5-x}Ta_xGe_4$ was found to exist at $0 < x < 1.0$ with the lattice parameters varying between $a = 7.2413(9)$, $c = 13.162(2)$ Å at $x = 0$ and $a = 7.1416(8)$, $c = 13.067(2)$ Å at $x = 1.0$. A small two-phase field separates this phase from monoclinic $Zr_{4-x}Ta_{1+x}Ge_4$, which exhibits a smaller homogeneity range of $0.1 < x < 0.4$. The respective lattice parameters vary between $a = 7.126(1)$, $b = 7.116(1)$, $c = 6.919(1)$ Å, $\beta = 109.350(3)°$ at $x = 0.1$ and $a = 7.076(5)$, $b = 7.062(2)$, $c = 6.890(6)$ Å, $\beta = 109.43(2)°$ at $x = 0.4$. Another small two-phase field separates this phase from orthorhombic $Zr_{2+x}Ta_{3-x}Ge_4$ with $0.1 < x < 1.1$, and lattice parameters vary between $a = 6.880(2)$, $b = 13.389(4)$, $c = 7.003(2)$ Å at $x = 1.1$ and $a = 6.810(4)$, $b = 13.20(2)$, $c = 6.929(3)$ Å at $x = 0.1$. The three phases therefore form a "phase bundle" that covers most of the composition range between binary Zr_5Ge_4 and $Zr_{2.1}Ta_{2.9}Ge_4$. It is remarkable that the volume per formula unit appears to vary in an almost linear fashion through the whole composition range, regardless of the actual structure of the compound (Fig. 3).

The new ternary compounds found in the Ge–Ta–Zr system meet the basic defining characteristics of phases stabilized by differential fractional site occupancy as they were given by Franzen and Köckerling (6); i.e., the individual metal atom sites are occupied by random mixtures of Zr and Ta and the site occupancies vary significantly from site to site (compare Table 2). For a better understanding of the observed site preferences, it is interesting to consider the local coordination of the different metal sites. The first coordination sphere of the three metal sites of monoclinic $Zr_{3.90}Ta_{1.10}Ge_4$ (first row) and orthorhombic

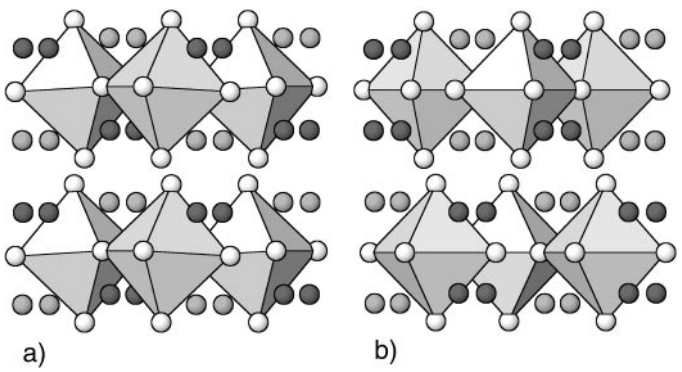

FIG. 2. (a) $Zr_{3.90}Ta_{1.10}Ge_4$, $P2_1/c$, view along [010] and (b) $Zr_{3.13}Ta_{1.87}Ge_4$, *Pnma*, view along [100]. Infinite layers of Ge octahedra are perfectly flat in the orthorhombic structure and twisted out of plane in the monoclinic structure.

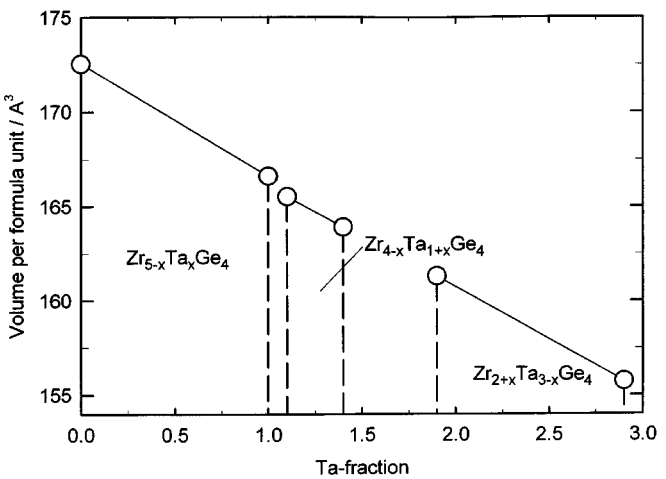

FIG. 3. Volume per formula unit $(Zr,Ta)_5Ge_4$ versus tantalum fraction. The graph also shows the extension of the different single phase fields as they were determined at 1450°C.

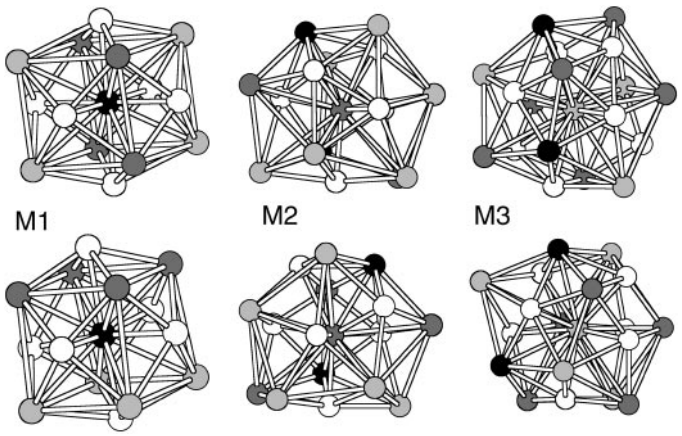

FIG. 4. Coordination polyhedra of the metal positions in $Zr_{3.90}Ta_{1.10}Ge_4$, $P2_1/c$ (above) and $Zr_{3.13}Ta_{1.87}Ge_4$, *Pnma* (below). White circles, Ge; light gray, *M*3; dark gray, *M*2; black, *M*1. Figures from left to right: *M*1, CN = 14; *M*2, CN = 16; *M*3 CN = 18.

$Zr_{2+x}Ta_{3-x}Ge_4$ (second row) including all neighbors at distances smaller than 3.9 Å is shown in Fig. 4.

One can see that the two phases $Zr_{3.90}Ta_{1.10}Ge_4$ and $Zr_{2+x}Ta_{3-x}Ge_4$ (and also the tetragonal phase $Zr_{5-x}Ta_xGe_4$, which is not included in Fig. 4) show the same principal type of coordination polyhedron: the position *M*1 is coordinated by 6 Ge atoms forming an octahedron capped by 8 metal atoms in a cubic arrangement yielding a coordination number of CN = 14. In contrast, *M*2 and *M*3 exhibit complicated coordination polyhedra with *M*2 surrounded by 6 Ge and 10 metal atoms (CN = 16) and *M*3 by 7 Ge and 11 metal atoms (CN = 18), respectively. In addition to the similarity in the type of coordination, the fractional site occupancies show the same trend in all three phases: position *M*1 always exhibits the highest Ta fraction, followed by position *M*2, while position *M*3 is essentially occupied by pure Zr.[2] This is consistent with the idea that the observed site preferences in these DFSO-stabilized compounds are strongly determined by the local coordination.

A more quantitative approach to understanding the connection between the chemical bonding at the metal site and the observed fractional site occupancy was successfully used in mixed Nb–Ta systems, using the total Pauling bond order as a measure of the metal–metal interaction at the different metal sites (5). In the current case, however, the application of the Pauling bond order is somewhat arbitrary, as the Pauling radii of Ta and Zr differ significantly. It was therefore decided to use Mulliken overlap populations and atomic orbital populations obtained by extended Hückel calculations as a measure of the chemical interactions and "site potentials" at the different metal sites.

Extended Hückel calculations were performed using the Caesar program package (21). The parameters used for the calculations are listed in Table 3. Parameters for Ge were taken from standard sources (21), while the parameters for Zr and Ta were obtained by solid-state charge iteration on binary Zr_5Ge_4 and on ordered Zr_4TaGe_4 using the structure of monoclinic $Zr_{3.90}Ta_{1.10}Ge_4$. Calculations were performed for all three crystal structures at the composition M_5Ge_4 discussed above using the experimentally obtained crystal structure data for $Zr_{3.90}Ta_{1.10}Ge_4$, $Zr_{3.13}Ta_{1.87}Ge_4$, and $Zr_{3.98}Ta_{1.02}Ge_4$ listed in Tables 1 and 2. As all of these compounds show fractional site occupancies, it was necessary to calculate different site occupancy models for the different phases.

Figure 5 shows the DOS curves for monoclinic $Zr_{3.90}Ta_{1.10}Ge_4$ and orthorhombic $Zr_{3.13}Ta_{1.87}Ge_4$ using the "idealized" occupancies (i.e., the site occupancy model closest to the experimentally determined site occupancies) of Ta on position *M*1 and Zr on position *M*2 and *M*3. The DOS curves of the two compounds exhibit very similar features, in agreement with the close structural relationships of the compounds discussed previously. The *s* states of Ge are situated at low energies (below -16 eV) and exhibit considerable mixing with the metal states. The *p* states of Ge are localized in broad blocks between approximately -12.5 and -10 eV also showing extended metal *s* and *p* contributions. The Fermi levels shown in Fig. 5 correspond to the real sample compositions of $Zr_{3.90}Ta_{1.10}Ge_4$ (74.2 electrons per unit cell) and $Zr_{3.13}Ta_{1.87}Ge_4$ (151.5 electrons per unit cell). The Fermi levels are situated in a block which consists predominately of the *d* states of the metals (Ta and Zr) corresponding to delocalized metal–metal bonds in the extended metal framework. Both compounds show a significant number of states at their

TABLE 3
Parameters Used in the Extended Hückel Calculations

Orbital	H_{ii}/eV	ζ_1	c_1	ζ_2	c_2
Zr, 5*s*	− 7.426	1.817			
Zr, 5*p*	− 4.740	1.776			
Zr, 4*d*	− 8.158	3.835	0.6213	1.505	0.5769
Ta, 6*s*	− 8.964	2.280			
Ta, 6*p*	− 5.243	2.241			
Ta, 5*d*	− 8.537	4.762	0.6815	1.938	0.6815
Ge, 4*s*	− 16.00	2.160			
Ge, 4*p*	− 9.00	1.850			

[2]A single crystal refinement of the Sm_5Ge_4-type phase at the composition $Zr_{2.29}Ta_{2.71}Ge_4$, $a = 6.815$, $b = 13.213$, $c = 6.928$ Å (which is almost the Ta-rich phase boundary of this phase) revealed the following site occupancies: *M*1 : 100% Ta, *M*2 : 83%, *M*3 : 3% Ta. It is thus not possible to realize the totally ordered ternary Sm_5Ge_4 type in the system Ge–Ta–Zr, as Ta starts to occupy the position *M*3 long before *M*2 is completely filled with Ta.

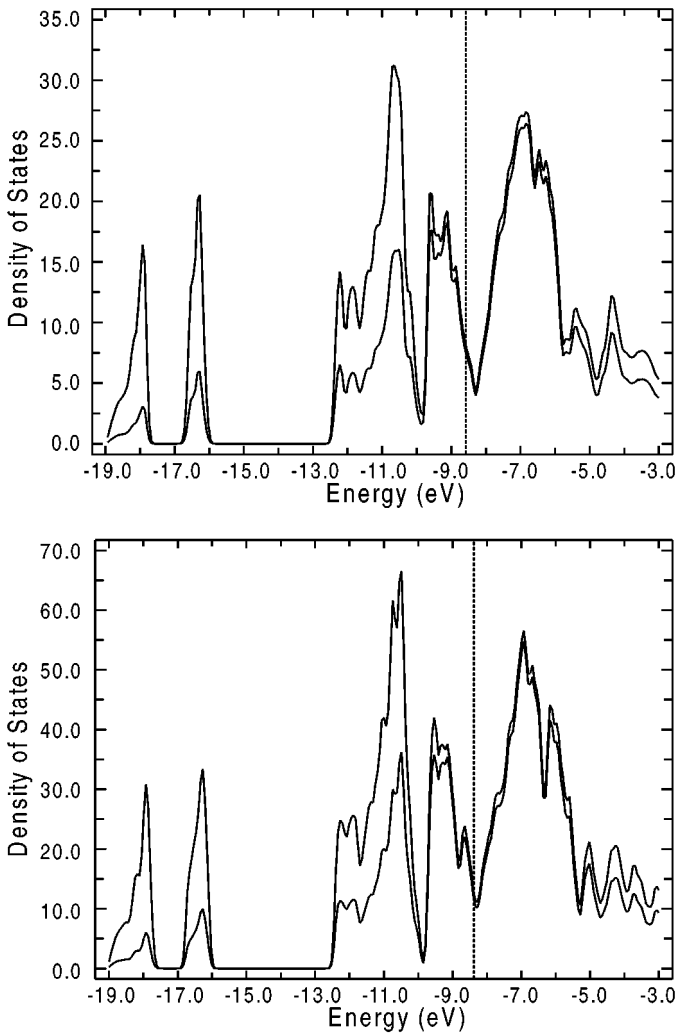

FIG. 5. Density of states for $Zr_{3.90}Ta_{1.10}Ge_4$, $P2_1/c$ (above) and $Zr_{3.13}Ta_{1.87}Ge_4$, *Pnma* (below). The inner lines are the metal (Zr and Ta) contributions to the DOS curves. The dashed line represents the Fermi level.

Fermi levels which are nevertheless situated near a local minimum in the *d* block.

Mulliken overlap populations (MOP) for the metal atoms were obtained from the extended Hückel calculations for the bonds of the first coordination sphere using all neighbors in the coordination polyhedra described previously (see Fig. 4). In a first step, the overlap populations for the different phases were calculated using the site occupancy model closest to the experimentally determined site occupancies. For the monoclinic phase for instance, this means Ta in position 1 and Zr in position 2 and 3 (see Table 2). This approach, however, gives only an approximation of the chemical bonding in the real phase where the metals are distributed randomly over the lattice sites *M*1 and *M*2. A possible way to overcome this problem and to find a better approximation for the description of the chemical bonding in the real phase is discussed here for the monoclinic phase $Zr_{3.90}Ta_{1.10}Ge_4$. Extended Hückel calculations were performed for all possible site occupancy models, i.e., for all possible permutations of Ta and Zr over the respective lattice sites *M*1 and *M*2, while *M*3 was taken as a pure Zr site in all models. The cumulated MOP's for each metal site were obtained from these calculations and the values were then used to define the overlap populations of a "weighed average model" using the actual refined site occupancies to determine the weighing factors. The results of these calculations for the monoclinic phase $Zr_{3.90}Ta_{1.10}Ge_4$ are listed in Table 4. The approach described above averages the total MOP according to the probability of a certain site occupancy situation to occur in the real crystal and may therefore (in the case of pronounced fractional site occupancies) be a more accurate tool to point out differences in the chemical bonding at different metal sites than the MOP obtained from only one single occupancy model, where differences in the MOP may also be due to the different sets of Extended Hückel parameters for the metals used in the calculations. In the current case, however, the observed differences between the averaged model and the "idealized" model (model A) are rather small (see Table 4), so the following discussion of the lattice site effects based on the simpler approach of the idealized models.

Table 4 shows a clear correlation between the observed site occupancies of the metal sites and the total MOP's of the respective site for the idealized model A as well as for the average model. This correlation may be attributed to the fact, that Ta as a group 5 element shows higher affinity to lattice sites that provide high overall bonding than Zr with only 4 valence electrons.

Cumulated Mulliken overlap populations were calculated for the three compounds characterized by single-crystal X-ray diffraction and a plot of the MOP's at different atomic sites versus the refined site occupations is shown in Fig. 6. The additional data set for the Sm_5Ge_4-type phase at the composition $Zr_{2.29}Ta_{2.71}Ge_4$[2] was included to demonstrate the effect of composition variations *within* the non-stoichiometric phases. Figure 6 shows a clear correlation between cumulated MOP's and fractional site occupancies. The plot shows the total MOP's (i.e., the sum of all MOP's in the first coordination sphere as shown in Fig. 4) as well as the sum of metal–metal MOP's. As mentioned before, the correlation of the cumulated MOP's with the tantalum fraction can be attributed to the additional valence electron

[2]A single crystal refinement of the Sm_5Ge_4-type phase at the composition $Zr_{2.29}Ta_{2.71}Ge_4$, $a = 6.815$, $b = 13.213$, $c = 6.928$ Å (which is almost the Ta-rich phase boundary of this phase) revealed the following site occupancies: *M*1 : 100% Ta, *M*2 : 83%, *M*3 : 3% Ta. It is thus not possible to realize the totally ordered ternary Sm_5Ge_4 type in the system Ge–Ta–Zr, as Ta starts to occupy the position *M*3 long before *M*2 is completely filled with Ta.

TABLE 4
Mullikan Overlap Populations for Various Site Occupancy Models for the Phase $Zr_{3.90}Ta_{1.10}Ge_4$, $P2_1/c$

Site occupancy model		Cumulated overlap population for the metal position		
		*M*1 (0.64 Ta/0.36 Zr)	*M*2 (0.23 Ta/0.77 Zr)	*M*3 (Zr)
Model A	Ta1, Zr2, Zr3	3.7772	3.4333	2.9477
Model B	Zr1, Zr2, Zr3	3.5891	3.4887	3.0001
Model C	Ta1, Ta2, Zr3	3.7082	3.5984	2.8329
Model D	Zr1, Ta2, Zr3	3.4855	3.6402	2.8860
Weighed average Model[a]	M1, M2, Zr3	3.6836	3.4901	2.9402

[a] MOP = 0.49*A + 0.28*B + 0.15*C + 0.08*D according to the observed site occupancies for $Zr_{3.90}Ta_{1.10}Ge_4$.

of Ta. The correlation of the metal–metal MOP's with the tantalum fraction may be explained by the fact, that 5*d* electrons of Ta are more delocalized than the 4*d* electrons of Zr, and Ta therefore prefers the lattice sites with higher (delocalized) metal–metal interactions. A similar effect has been reported for several mixed Nb/Ta compounds (5).

Figure 6 demonstrates that the observed site occupancies of the different phases can be understood in terms of the differential fractional site occupancy concept using the Mulliken overlap populations as a measure for differences in the chemical bonding at different lattice sites. The two ternary phases can thus be regarded as DFSO-stabilized compounds, and the curves in Fig. 6 appear to show a quantitative relationship between a certain amount of chemical bonding at the lattice site (here represented by cumulated MOP's) and a certain Ta/Zr fraction forming an "ensemble averaged metal" at the lattice site. This relationship appears to be valid for the entire investigated $(Zr,Ta)_5Ge_4$-composition range, regardless of the actual structure formed or the actual lattice site involved (the data points in Fig. 6 belong to nine different coordination spheres in three different structure types).

A different approach to consider the observed site preferences, was recently reviewed by Miller (22) who demonstrated the usefulness of atomic orbital populations obtained by Extended Hückel calculations in the understanding of "coloring problems" in solids. According to Miller, atomic orbital populations can be regarded as a measure of the "site energy" the value of which is sensitive for the degree of charge transfer between the atoms as well as for the coordination geometry at each site. Results of atomic orbital population analyses of homonuclear structures can thus be used to understand site preferences in heteronuclear structures. In order to test the possible use of this approach for the current problem, the respective atomic orbital populations for all four compounds were obtained by extended Hückel calculations using occupancy models with Zr on all three metal positions.

The results are shown in Fig. 7, where the atomic orbital populations are plotted versus the observed fractional occupancy of the respective site. The correlation of the values is strong, showing the preference of the more electronegative Ta for lattice sites with higher atomic orbital population.

CONCLUSIONS

The two new ternary phases $Zr_{4-x}Ta_{1+x}Ge_4$ and $Zr_{2+x}Ta_{3-x}Ge_4$ form, together with the solid solution of Ta in binary Zr_5Ge_4 ($Zr_{5-x}Ta_xGe_4$), a "bundle" of structurally closely related phases which covers most of the composition range between Zr_5Ge_4 and $Zr_{2.1}Ta_{2.9}Ge_4$. These phases show features typical for DFSO-stabilized compounds, i.e., fractional site occupation between Zr and Ta on the metal sites combined with strong differences in the Zr/Ta ratio from site to site. It is possible to understand the observed site preferences by a correlation of the fractional occupancies with the "bond energies" at the respective site repre-

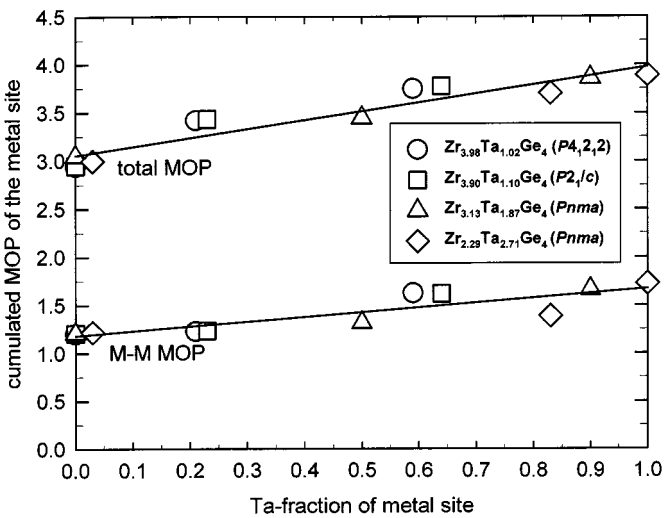

FIG. 6. Cumulated MOPs versus fractional site occupation for all metal sites of four different $(Zr,Ta)_5Ge_4$ compounds. The upper curve shows the total MOPs for the first coordination spheres and the lower curve shows only the metal–metal contributions. The extended Hückel calculations were performed using idealized occupancy models (see text).

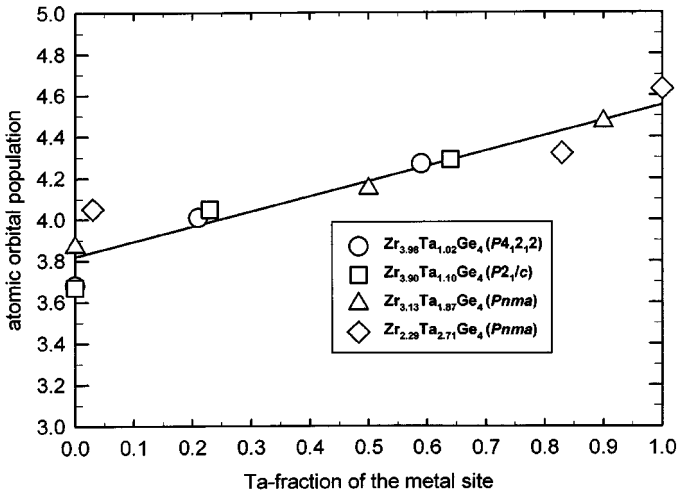

FIG. 7. Atomic orbital populations versus fractional site occupancies for all metal sites of four different $(Zr,Ta)_5Ge_4$ compounds. The extended Hückel calculations were performed using Zr parameters for all metal atoms.

sented by the cumulated Mulliken overlap populations of the first coordination sphere. According to this figure, Ta will preferably occupy sites with higher overall MOP (due to its additional valence electron) as well as lattice sites with higher metal–metal MOP (according to the more delocalized character of the 5*d* electrons compared to the 4*d* electrons of Zr). A similar correlation was found to exist between the site energies represented by the atomic orbital population (22) and the fractional occupancies. Due to the relative similar properties of Ta and Zr, however, these site preferences do not yield in completely ordered ternary compounds as they were reported for isostructural compounds in lanthanide and actinide systems (13–16), but rather in partially ordered, nonstoichiometric compounds.

It should be mentioned that the original DFSO concept was formulated based on phases exhibiting rather limited composition ranges. This fact led to the idea that the random mixtures of metals were forming "ensemble averaged metals" optimized for the amount of chemical bonding provided by the respective lattice site in the structure (6). The compounds described in the current study, however, show extended composition ranges (variation of the Ta/Zr ratio), which means that the phases are able to adapt to the variation of the overall Ta/Zr ratio by a variation of the actual fractional site occupancies, without loosing the general feature of strong site preferences. The continuous variations in the fractional site occupancies are here accompanied by a continuous variation of the lattice parameters (and to a lesser extent also the atomic positions) yielding changes in the bond energies within the coordination spheres. Phase transitions into closely related neighboring phases, such as in the Ge–Ta–Zr system, are only triggered if the range of continuous variation within a single structure is exceeded. As DFSO-stabilized phases with noticeable composition ranges have also been reported in other systems (23, 24), it may in fact be assumed that this more general DFSO mechanism is quite common among mixed early transition metal compounds. The application of this generalized DFSO concept may be a valuable tool, not only for the prediction of new ternary and multinary compounds in similar systems, but also for the estimation of site preferences based upon calculated Mulliken overlap population in systems, where such data are not readily available.

ACKNOWLEDGMENTS

K.R. thanks the Austrian Science Foundation (FWF) for an Erwin-Schrödinger Scholarship. This research was supported by the Office of the Basic Energy Science, U.S. Department of Energy. The Ames Laboratory is operated by the DOE under Contract W-7405-Eng-82.

REFERENCES

1. X. Yao and H. F. Franzen, *J. Solid State Chem.* **86,** 88 (1990).
2. X. Yao and H. F. Franzen, *Z. Anorg. Allg. Chem.* **598,** 353 (1991).
3. X. Yao and H. F. Franzen, *J. Am. Chem. Soc.* **113,** 1426 (1991).
4. X. Yao, G. J. Miller, and H. F. Franzen, *J. Alloys Comp.* **183,** 7 (1992).
5. X. Yao, G. A. Marking, and H. F. Franzen, *Ber. Bunsenges. Phys. Chem.* **96,** 1552 (1992).
6. H. F. Franzen and M. Köckerling, *Prog. Solid State Chem.* **23,** 265 (1995).
7. G. A. Marking and H. F. Franzen, *J. Am. Chem Soc.* **115,** 6126 (1993).
8. J. Cheng and H. F. Franzen, *J. Solid State Chem.* **121,** 362 (1996).
9. Yu. D. Seropegin and M. V. Rudometkina, *J. Less-Common Met.* **135,** 127 (1987).
10. M. V. Rudometkina, Yu. D. Seropegin, and E. E. Schvyryaeva, *J. Less-Common Met.* **138,** 263 (1988).
11. Bruker AXS, Ltd., and G. M. Sheldrick, "Bruker AXS PAK," 1998.
12. O. I. Bodak, Yu. K. Gorelenko, V. I. Yarovets, and R. V. Skolozdra, *Inorg. Mater.* (*transl. Izv. Akad. Nauk. SSSR*) **20,** 741 (1984).
13. T. Le Bihan and H. Noël, *J. Alloys Comp.* **227,** 44 (1995).
14. P. Villars and L. D. Calvert (Eds.), "Pearsons Handbook of Crystallographic Data for Intermetallic Phases," 2nd ed. ASM, 1991.
15. T. Le Bihan, K. Hiebl, P. Rogl, and H. Noël, *J Alloys Comp.* **235,** 80 (1996).
16. T. Le Bihan, H. Noël, and P. Rogl, *J. Alloys Comp.* **213,** 540 (1994).
17. Yu. D. Seropegin, O. I. Bodak, I. A. Guseva, and L. A. Panteleimenov, *Moscow Univ. Chem. Bull.* **35,** 111 (1980).
18. Yu. O. Seropegin, V. V. Tabachenko, and M. G. Mys'kiv, *Sov. Phys. Crystallogr.* **29,** 95 (1984).
19. P. I. Krypyakevich and V. A.Yartys, *Dopov. Akad. Nauk. Ukr. RSR Ser. A* **12,** 1129 (1975).
20. J. Le Roy, J. -M. Moreau, D. Paccard, and E. Parthé, *Acta Crystrallogr. Sect. B* **34,** 3315 (1978).
21. J. Ren, W. Liang, and M. -H. Whangbo, "CAESAR." Prime Color Software Inc., North Carolina State University, 1998.
22. G. J. Miller, *Eur. J. Inorg. Chem.*, 523 (1998).
23. H. Kleinke and H. F. Franzen, *J. Am. Chem. Soc.* **119,** 12824 (1997).
24. H. Kleinke, *Chem. Commun.* **20,** 2219 (1998).